The following publication L. Dang et al., "Tunable Hz Intrinsic Linewidth Single-Polarization Linear Cavity Fiber Laser Based on Parity-Time Symmetric Optics With a High-Q Microresonator," in Journal of Lightwave Technology, vol. 43, no. 18, pp. 8849-8856, 15 Sept.15, 2025 is available at https://doi.org/10.1109/JLT.2025.3590173.

Tunable Hz intrinsic linewidth single-polarization linear cavity fiber laser based on parity-time symmetric optics with a high-Q microresonator

Laiyang Dang, Dongmei Huang, *Member, IEEE*, Wenhao Zhu, Feng Li, *Senior Member, IEEE*, Xiaofan Zhang, Zhenda Xie, and Kunpeng Jia

Abstract-High-performance tunable fiber laser with ultranarrow linewidth and single polarization is driving the progress in fundamental research and engineering applications. However, it is still challenging to achieve single polarization tunable fiber laser due to the redundant laser cavity and the lack of polarization selectivity of ordinary optical fibers. Here, we propose and demonstrate a novel scheme for the generation of an ultra-narrow linewidth and single polarization linear cavity fiber laser based on parity-time (PT) symmetry in combination with a high-Q Fabry Pérot (FP) resonator. The PT symmetry can be achieved between two subspaces in a single physical loop based on optical polarization diversity and controllability. Benefitting from the FP resonator with a high Q factor of 10⁷, the measured laser side mode suppression ratio reaches 73.3 dB and the high frequency white noise floor is ~2.62 Hz²/Hz, corresponding to an intrinsic linewidth of about 8.2 Hz. The laser output has a high polarization extinction ratio of ~35.46 dB and its maximum output power fluctuation is less than 1.6% over more than 60 min due to the high polarization sensitivity of the FP resonator. The wavelength tuning range is 52.15 nm (from 1523.95 to 1576.1 nm), covering the entire flat region of the erbium doped gain fiber. The proposed PT-symmetric system realizes an ultranarrow linewidth and single-polarization tunable singlefrequency fiber laser in a robust and efficient way, which provides a new insight to improve the performance of other laser

Index Terms—Tunable fiber laser, ultra-narrow linewidth, single polarization, parity-time symmetry, high-Q microresonator.

This work is financially supported by the National Natural Science Foundation of China (62105274), the Research Grants Council, University Grants Committee of Hong Kong SAR (PolyU15301022), the Innovation Commission of Shenzhen Municipality (JCYJ20210324133406018), the National Key R&D Program of China (2023YFB2805700), and the Program of Jiangsu Natural Science Foundation (BK20230770, BK20232033). (Corresponding author: Dongmei Huang; Kunpeng Jia.)

Laiyang Dang, Dongmei Huang, and Wenhao Zhu are with the Photonics Research Institute, Department of Electrical and Electronic Engineering, The Hong Kong Polytechnic University, Hong Kong, and also with the The Hong Kong Polytechnic University Shenzhen Research Institute, Shenzhen 518057, China (e-mail: laiyang.dang@polyu.edu.hk; meihk.huang@polyu.edu.hk; wenhao.zhu@connect.polyu.hk).

Feng Li is with the The Hong Kong Polytechnic University Shenzhen Research Institute, Shenzhen 518057, China (e-mail: lifeng.hk@gmail.com).

Xiaofan Zhang, Zhenda Xie, Kunpeng Jia are with the National Laboratory of Solid State Microstructures, School of Electronic Science and Engineering, and Collaborative Innovation Center of Advanced Microstructures, Nanjing University, Nanjing 210093, China (e-mail: dz20230028@smail.nju.edu.cn; xiezhenda@nju.edu.cn; jiakunpeng@nju.edu.cn).

I. Introduction

Cingle-polarization and single-frequency lasers with narrow Ulinewidth, low noise and high stability have driven the applications in microwave optics, coherent communications, and precision metrology [1]-[6]. Owing to the broad gain bandwidth of the laser cavity, which is larger than the cavity mode interval, longitude mode management is required to realize single frequency operation [7]–[11]. Researchers have proposed various kinds of methods including reducing the cavity length, optical feedback and parity-time (PT) symmetry to realize laser mode selection. A narrow bandwidth of megahertz is required to achieve single mode operation as the cavity length is on the order of tens of meters [12], which increases the difficulties in the fabrication and control of stability. Reducing the cavity length to increase the free spectrum range (FSR) such as employing an ultra-compact cavity implemented by a pair of mirrors or a distributed feedback (DFB) phase-shift grating can ensure single mode operation [13], [14], but it is complex for the manufacturing and challenging to realize wavelength tuning. Besides, a very high gain is required to reach the threshold of lasing. The mode selected by external optical feedback can also be used to enhance the gain competition of modes in the cavity, resulting in a strong optical oscillation or lasing of the unique mode This mechanism provides a flexible and controllable mode selection approach, but the feedback must be precisely designed to achieve effective mode selection, and its stability is easily affected by the temperature or variation of the environment. A novel concept PT symmetry is introduced to the photonic system to realize mode selection due to PT symmetry breaking [18]-[23]. Two mutually coupled optical loops are required to build up a PT symmetry system, where the balance between gain and loss is adjusted to control the PT symmetry breaking point and select the desired mode for single mode operation in the laser cavity. In principle, the desired mode will have a higher gain, while the other modes can be suppressed in the PT symmetry breaking point. Based on PT symmetry, a single mode laser has been demonstrated operating around an exceptional point [24], [25]. Besides, widely wavelength tunable fiber ring laser and an integrated wavelength tunable single mode microring laser have been realized based on PT symmetry [26], [27]. However, these proposed single mode lasers or wavelength tunable lasers have

© 2025 IEEE. Personal use of this material is permitted. Permission from IEEE must be obtained for all other uses, in any current or future media, including reprinting/republishing this material for advertising or promotional purposes, creating new collective works, for resale or redistribution to servers or lists, or reuse of any copyrighted component of this work in other works.

relatively low side mode suppression ratio (SMSR) less than 45 dB and are not operating in single polarization.

Single mode laser normally operates in eigenpolarization modes with different wavelengths due to the birefringence of the ordinary fiber, which introduces power fluctuations and limits its applications. Therefore, stable single mode as well as single polarization laser is desirable in many special applications. Various techniques have been proposed to obtain single polarization laser such as introducing a polarization dependent phase shifter [28], self-injection locking with polarization selective feedback [29], external high Q fiber ring [30] et al. However, it is challenging to tune the wavelength due to polarization dependent of the wavelength. How to realize a highly stable single frequency and single polarization wavelength tunable laser with high SMSR and high polarization extinction ratio (PER) is desirable and challenging.

In this paper, we propose and experimentally demonstrate a stable tunable ultra-narrow linewidth and single-polarization linear cavity fiber laser based on PT symmetric optics with a high-Q Fabry Pérot microresonator (FPMR). The FPMR can enlarge the mode interval to reduce the number of longitudinal modes, and the high Q characteristic can also improve the restriction of longitudinal modes to weaken the mode hopping in the laser cavity. The PT symmetry is realized by adjusting the coupling coefficient between the clockwise (CW) and counterclockwise (CCW) light waves in the FPMR. Controlling the polarization mode of the FPMR will change the coupling coefficient to maintain or break the PT symmetry condition for mode selection to achieve single mode operation. Besides, the FPMR and the PT symmetry condition are both sensitive to the polarization state, which will ensure single polarization operation. Based on PT symmetric optics with a high Q factor FPMR, a state-of-the-art continuously tunable single-frequency laser with a SMSR of 73.3 dB, PER of 35.64 dB and a wavelength tunable range from 1523.95 to 1576.1 nm is realized. Experimental results show that the proposed laser scheme exhibits a low white frequency noise floor of \sim 2.62 Hz²/Hz, corresponding to an intrinsic linewidth of \sim 8.2 Hz, and a relative intensity noise (RIN) of -140.3 dB/Hz. The maximum fluctuations of the output power, wavelength and the PER in a long-term are less than 0.043 mW, 0.004 nm and 3.06 dB, respectively, indicating that the laser exhibits high stability.

II. THEORETICAL ANALYSIS

A typical scheme of PT symmetry with nested a FPMR for single-frequency operation is shown in Fig. 1(a). The proposed linear laser configuration is a double-ring cascaded resonant system, which consists of an external long fiber cavity for laser mode generation and a built-in FPMR for optical mode selection. It is worth mentioning that the FSR of the two resonators must be strictly controlled so that the resonance peaks of the corresponding resonators will overlap to achieve stable laser operation. A schematic diagram of the mode matching principle of two resonant cavities is presented in Fig. 1(b). The laser oscillation frequency f should

simultaneously satisfy the external linear cavity and the resonance condition of the FPMR [31]:

$$f = f_{MR} = N \times f_{LC} \tag{1}$$

where f_{MR} is the FSR inside the FPMR, and f_{LC} is the FSR of the external long laser cavity. The variable N is an integer that represents the multiplier of the mode spacings of the FPMR and the external linear cavity. Besides, a high-Q FPMR is required so that the full-width at half maximum of the nested cavity must be smaller than the mode spacing of the external linear cavity to ensure single-mode filtering and thus improve the mode suppression capability of the PT symmetric system. Subsequently, the internal resonant cavity functions as a spectral filter, effectively reducing the number of modes and improving laser stability, and the polarization states of the bidirectionally transmitted resonant modes in the internal optical cavity can be controlled when these conditions are satisfied.

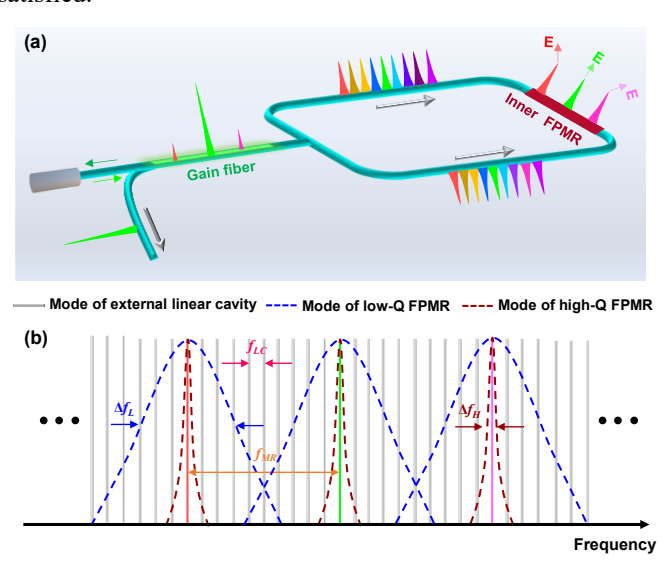


Fig. 1. (a) Scheme for single-frequency PT-symmetric linear fiber cavity laser generation based on nested FPMR. (b) Distribution of various modes in the proposed laser cavity. The FSR of the external linear cavity is represented by f_{LC} (gray curve), and the FSR of the FPMR is represented by f_{MR} (orange curve). Full widths at half maximum of the low- and high-Q FPMR are denoted by Δf_L (blue curve) and Δf_H (dark red curve), respectively.

It should be noted that when the bandwidth of the tunable band-pass filter (TBPF) is greater than the mode spacing of the FPMR, a small number of super-modes whose gain exceeds the laser threshold will be excited. In such case, these different laser modes are oscillated simultaneously, resulting in multi-longitudinal mode (MLM) operation of the laser. Here, the light propagating in a single FPMR has reciprocity, and two counter-propagating light waves can be used to create a PT-symmetric dual-polarization controllable physical loop, one of which provides gain from the EDF and the other of which introduces the loss. PT symmetry is an important mechanism for describing the symmetry of non-Hermitian quantum systems. Its core is the invariance of the system under the joint operation of parity (P) and time reversal (T). Traditional quantum mechanics requires the Hamiltonian to be Hermitian to ensure real energy eigenvalues, while PT symmetry allows non-Hermitian Hamiltonians to still have

real energy spectra when they satisfy the PT symmetric phase (system parameters (such as gain/loss) are below a critical value, the eigenvalues are real and the system is in a stable state) and the PT symmetry breaking phase (after exceeding the critical value, the eigenvalues become complex conjugate pairs, and the system exhibits a dynamic imbalance of gain and loss). The realization of PT symmetry in optical systems relies on the symmetrical distribution of gains and losses in the spatial or modal dimension. In a single physical loop, two light waves with orthogonal polarization states form periodic coupling through the birefringence effect. This coupling causes the different polarization components to experience alternating net gain and loss regions when propagating in the cavity. Here, A series of resonant modes are produced at the same frequency due to the inconsistent FSR of the two resonators. Based on this, the resonant modes will interact at equivalent frequencies, and the time-domain coupling mode equation of the *n*-th modes of the single-ring PT-symmetric laser is given by [32], [33]

$$\frac{d}{dt} \begin{bmatrix} G_n \\ L_n \end{bmatrix} = \begin{bmatrix} -i\omega_n + g_{G_n} & i\kappa_n \\ i\kappa_n & -i\omega_n + \alpha_{L_n} \end{bmatrix} \begin{bmatrix} G_n \\ L_n \end{bmatrix}$$
 (2)

in which G_n and L_n represent the field amplitudes of n-th modes in two coupled net gain and loss subspaces, respectively. ω_n is the intrinsic angular frequency of the laser system without PT symmetry, g_{Gn} and α_{Ln} represent the gain and loss coefficients of the n-th modes determined by the EDF gain and the inherent loss of the laser cavity. κ n is the coupling coefficient between the two counter-propagating subspaces. Therefore, according to the coupled mode Eq. (2), the eigenfrequencies of the two supermodes can be represented as follows when the system is PT symmetric

$$\omega_n^{(G,L)} = \omega_n + i \frac{g_{G_n} + \alpha_{L_n}}{2} \pm \sqrt{\kappa_n^2 - \left(\frac{g_{G_n} + \alpha_{L_n}}{2}\right)^2}$$
 (3)

The PT symmetry condition in which the gain and loss coefficients have the same value $(g_{Gn} = -a_{Ln})$ can be achieved by adjusting the polarization modes of the FPMR, and Eq. (3) can be simplified to

$$\omega_n^{(G,L)} = \omega_n \pm \sqrt{\kappa_n^2 - g_{G_n}^2} \tag{4}$$

Here, the relationship between the real and imaginary parts of the normalized eigenfrequencies and the ratio between the gain and the coupling coefficient can be obtained from the above equation, as shown in Figs. 2(a) and 2(b). A critical situation occurs when gain/loss equals the coupling coefficient, which is defined as an exceptional point (EP). In this case, two originally independent light modes (such as different frequencies or polarizations) are completely merged, showing a degeneracy of frequency and loss rate, that is, the two are exactly the same. When $g_{Gn} < \kappa_n$, the system is a strong coupling region where the PT symmetry is not broken, and mode splitting will occur at the eigenfrequency. When $g_{Gn} > \kappa_n$, there is a weak coupling region that satisfies the PT symmetry breaking condition, that is, there is a conjugate mode pair in which one mode is amplified, one mode is attenuated, and the other modes are neutral.

Moreover, the gain of the main mode exceeds the oscillation threshold, while the gain of other modes is lower than the oscillation threshold, and SLM operation of long-cavity fiber lasers can also be realized. The maximum gain contrast can be expressed as

$$g_{\text{max}} = g_{G0} - g_{G1} \tag{5}$$

where, g_{G0} and g_{GI} are the gain coefficients of the main mode and the adjacent mode, respectively. Generally, the gain difference g_{max} is quite small, thus placing very strict requirements on the 3-dB bandwidth of the tunable TBPF to achieve stable SLM lasing, as illustrated in Fig. 2(c). In the PT symmetric laser system, the gain contrast can be defined as

$$g_{\text{max}_PT} = \sqrt{g_{G0}^2 - g_{G1}^2} \tag{6}$$

The gain contrast ratio, also known as the gain enhancement factor, is further calculated to evaluate the degree of improvement in mode selection, given by

$$\Upsilon = \frac{g_{\text{max}_PT}}{g_{\text{max}}} = \sqrt{\frac{g_{G0}/g_{G1} + 1}{g_{G0}/g_{G1} - 1}}$$
(7)

In this PT-symmetric laser system, the gain contrast is dramatically enhanced, which intensifies the gain competition effect between longitudinal modes. Figure 2(d) illustrates the principle of PT symmetry after preliminary model selection through FPMR, which can achieve SLM operation with high stability.

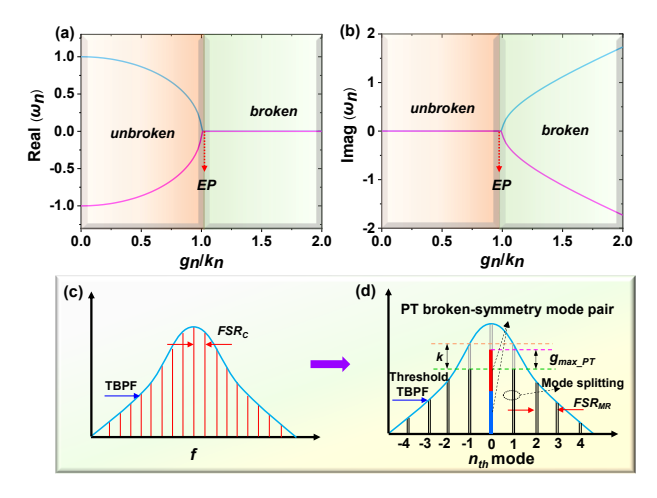


Fig. 2. Numerical analysis of the (a) real and (b) imaginary parts of the normalized eigenfrequencies of a single cavity PT-symmetric system. The gain contrast principle of various order modes in (c) conventional laser system without FPMR and (d) PT-symmetric laser system with FPMR.

In non-Hermitian systems, the mode degeneracy of the EP region can enhance mode selective coupling through phase matching. When the laser mode is coupled with a high-Q FP resonant cavity in the EP region, the gain of a specific longitudinal mode is significantly enhanced, while other longitudinal modes are strongly suppressed due to mode competition. Compared with conventional cavity frequency coupling, the asymmetric coupling mechanism between the laser mode and the microresonator mode in the EP region is more suitable for single longitudinal mode and narrow linewidth requirements. Moreover, the subharmonic entrainment phenomenon of the high-Q FP cavity originates from the periodic response of the resonant cavity to the laser phase noise, which easily leads to

subharmonic frequency locking. EP coupling destroys the symmetry of the system, making the subharmonic components unable to meet the phase matching conditions, thereby avoiding the entrainment effect [32].

III. EXPERIMENTAL SETUP

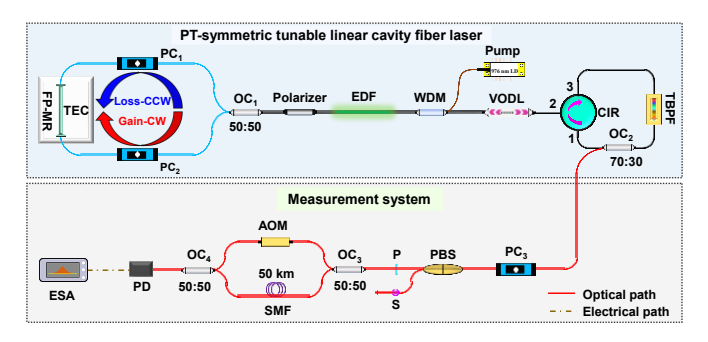


Fig. 3. Experimental setup of the proposed PT-symmetric tunable linear cavity fiber laser induced by an optical fiber FP-MR and DSHI measurement system. EDF, erbium-doped fiber; FPMR, Fabry-Pérot microresonator; TEC, thermoelectric cooler; OC, optical coupler; PC, polarization controller; WDM, wavelength division multiplexer; TBPF, tunable bandpass filter; VODL, variable optical delay line; CIR, circulator; PBS, polarization beam splitter; SMF, single-mode fiber; AOM, acousto-optic modulator; PD, photodetector and ESA, electrical spectrum analyzer.

The experimental setup of the proposed tunable single frequency all-fiber laser system and the measurement system is schematically illustrated in Fig. 3. The PT symmetric photonic system is achieved by a single ring structure containing a high-Q FPMR and a 3-dB optical coupler 1 (OC₁), where the clockwise and counterclockwise light waves coupled with each other. The polarization states of the CW and CCW light waves are adjusted by two polarization controllers (PC1 and PC2) to balance the gain and loss in the FPMR. The pump light is injected into a 50-cm-long erbiumdoped fiber (Liekki, Er80-8/125) through a 980/1550-nm wavelength division multiplexer (WDM). A polarizer is inserted into the active cavity to suppress mode hopping and ensure single polarization. A variable optical delay line (VODL) is employed to control the relative position of the laser cavity modes with respect to the FPMR's modes. The thermoelectric cooler (TEC) is to control the temperature of FPMR to ensure the stability of PT symmetry. The circulator (CIR) combined with a single-pass tunable band-pass filter (TBPF) is used to select and tune the wavelength of the linear cavity laser. The 30% port of OC₂ is used to monitor the output laser and the 70% port is recycled to the laser cavity. In the measurement system, the laser is inserted into the fiber polarization beam splitter (PBS), and the orthogonal polarization eigenmode is characterized by adjusting the PC3. The delayed self-heterodyne interferometry (DSHI) system is used to characterize the radio-frequency (RF) spectrum and frequency noise of the proposed laser. Two 3-dB couplers (OC₃ and OC₄) are utilized to construct a Mach-Zehnder interferometer. Herein, one arm generates optical delay via a 50 km single-mode fiber (SMF), and the other arm uses an acousto-optic modulator (AOM) to shift the frequency by 80 MHz. A photodetector (PD) and an electrical spectrum

analyzer (ESA, N9020B, KEYSIGHT) are used to detect and analyze the beat signal from the MZI. The spectra of the tunable single frequency laser are measured by an optical spectrum analyzer (OSA, ANDO, AQ-6315B) with a resolution of 0.05nm.

IV. EXPERIMENTAL RESULTS AND DISCUSSION

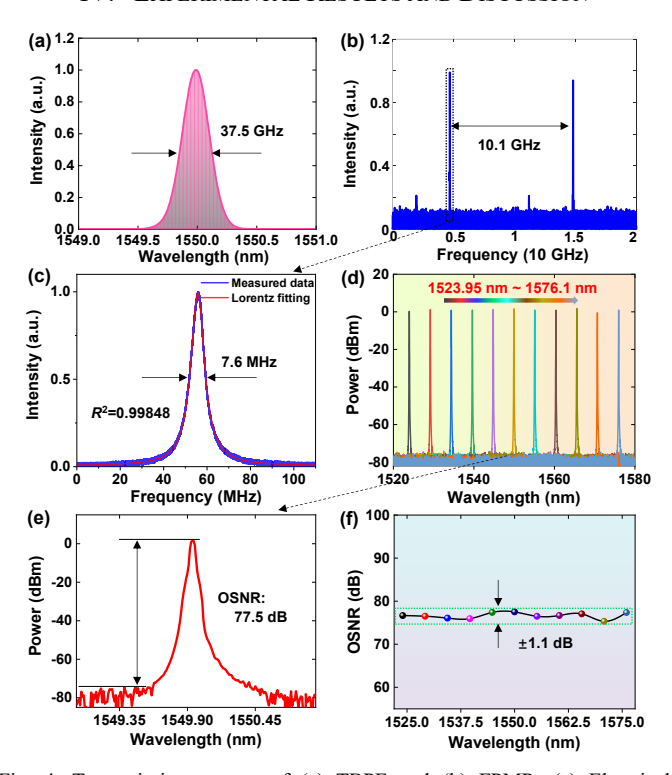


Fig. 4. Transmission spectra of (a) TBPF and (b) FPMR. (c) Electrical spectrum of a single comb tooth. (d) Spectral evolution when the filter is tuned. (e) Spectral shape around 1549.94nm. (f) OSNRs fluctuation under different wavelength channels.

Figure 4(a) shows the output spectrum of the TBPF to demonstrate the filtering performance. The output spectrum exhibits a good Gaussian shape and a 3-dB bandwidth of 37.5 GHz. The transmission spectrum of the FPMR is measured using a commercial swept laser, with an FSR of 10.1 GHz as shown in Fig. 4(b). The linewidth of the FPMR is 7.6 MHz, and the corresponding quality (Q) factor is 2.5×10^7 , as shown in Fig. 4 (c). Hence, the FPMR used in the experiment has an extremely narrow bandwidth, which can ensure that a small number of external linear cavity longitudinal mode can be filtered out in each comb tooth to achieve effective PTsymmetric mode selection and suppress laser mode hopping. SLM lasing of laser cannot be achieved through narrow-band filtering since the bandwidth of TBPF is larger than the FSR of FPMR. However, as shown in Fig. 4(d), the single wavelength is achieved, indicating that PT symmetry will further help realize mode selection. By tuning the central wavelength of the TBPF, a tunable single frequency laser is realized, ranging from 1523.95 nm to 1576.1 nm, completely covering the entire gain flat region of the EDF. In addition, the 3 dB bandwidth of the filter is 37.5 GHz, which is larger than the FSR (10.1 GHz) of the FPMR and includes resonant cavity modes at any tuning wavelength. Moreover, no gaps or inaccessible wavelengths are observed within the range of 52.15 nm, confirming seamless coverage. Although there are discrete cavity modes, the dense mode spacing allows the laser to transition smoothly between

wavelengths without significant interruptions. In addition, the devices used, especially the micro-resonators, maintain good transmission performance in the tuning range. Therefore, there is no breaking during whole tuning range. The spectrum with a central wavelength of 1549.94 nm is shown in Fig. 4(e), where the OSNR is as high as 77.5 dB with a good spectral line shape due to the high Q factor of the FPMR. The optical signal-to-noise ratio (OSNR) for different wavelengths is also characterized and its fluctuation is less than ± 1.1 dB, which is shown in Fig. 4(f). This proposed tunable single frequency laser has high performance with a wide tuning range, and the wavelength tuning range can be further extended if a doped fiber with a broader gain is available.

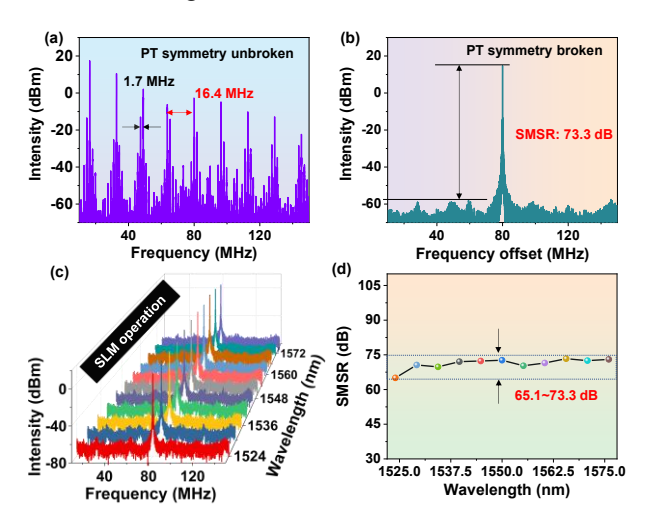


Fig. 5. RF spectra measured by the delayed self-heterodyne method of the PT symmetric fiber laser under (a) PT symmetry unbroken and (b) PT symmetry broken. (c) RF spectra corresponding to the tuning wavelength. (d) Fluctuations of SMSR at different wavelengths.

Based on theoretical analysis, it can be obtained that PT symmetry can suppress the side mode of MLM lasers. In our experimental system, the polarization state of light bidirectionally passing through the FPMR is adjusted to verify whether PT symmetry can suppress the side mode of the MLM laser to establish single-frequency laser output. To further study the characteristics of longitudinal modes for different operating states and different wavelengths in the PTsymmetric laser system, the RF spectra are measured by selfheterodyne method, as shown in Fig. 5. At a wavelength of 1549.94 nm, the RF spectrum with PT symmetry unbroken is shown in Fig. 5(a), from which we can infer that the laser operates in MLM oscillations. The large frequency spacing of 16.4 MHz is much smaller than the FSR of the FPMR. It is worth noting that light propagating in CW and CCW directions will form Sagnac interference. Therefore, a modulation phenomenon occurs in the MLM RF spectrum of the laser [26], [34], [35]. Additionally, the small frequency spacing of 1.7 MHz results from the FSR of the long-cavity MLM laser. By finely adjusting the polarization state of the CW and CCW light waves in the FPMR, the gain and loss can satisfy the PT symmetry broken condition, and the corresponding RF spectrum of the beat signal is shown in Fig. 5(b). Here, no beat frequency signal is observed except for the 80 MHz frequency shift component in the span of 140 MHz, which proves that the PT symmetric system induced by FPMR has excellent mode selectivity. The RF spectra of different single wavelength lasers are shown in Fig. 5(c). It indicates that the PT symmetric optics-based single frequency laser maintains a stable SLM lasing for the wavelength tuning

process. Figure 5(d) shows the SMSR disturbance of the laser for different wavelengths, ranging from 65.1~73.3 dB due to the net gain difference in the laser cavity. In the experiment, the length of the VODL is adjusted to match the mode of the laser cavity and the micro-resonator, and the PT symmetry breaking is better used to suppress the longitudinal mode of the laser to realize the SLM operation. In addition, the temperature control of the FPMR is realized by TEC, and the whole experimental system is placed on the constant temperature and vibration isolation platform, and no obvious mode hopping phenomenon is observed in the absence of external noise interference.

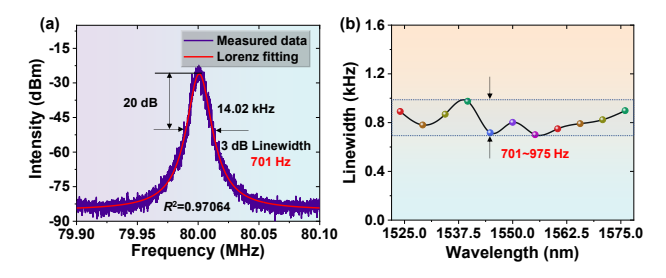


Fig. 6. (a) Optical self-heterodyne beat frequency spectrum under the laser wavelength of 1550.2 nm. (b) 3-dB linewidth at different tuning wavelengths obtained by Lorentz fitting.

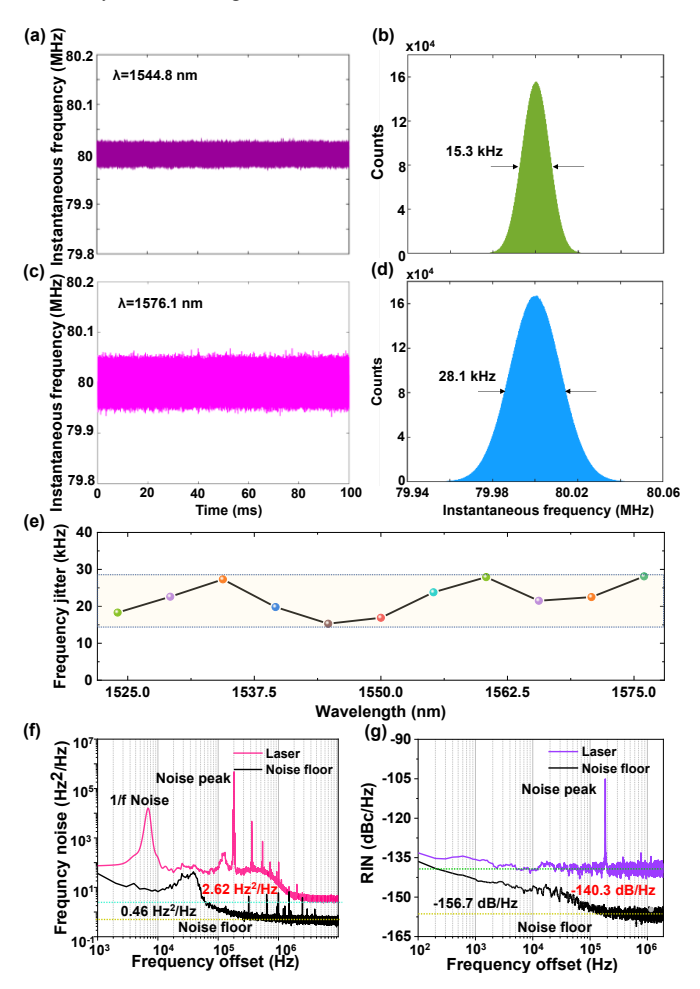


Fig. 7. (a) Instantaneous frequency of the laser wavelength is tuned to 1544.8 nm. (b) Distribution of instantaneous frequency at 1544.8 nm. (c) Instantaneous frequency of the laser wavelength is tuned to 1576.1 nm. (d) Distribution of instantaneous frequency at 1576.1 nm. (e) Frequency jitter fluctuation of laser under different wavelength conditions. (f) Frequency noise and (g) RIN spectra of the fiber laser.

The linewidth characteristics of the fiber laser under PT-symmetry condition is then evaluated by the DSHI measurement system. The self-heterodyne beat signal is detected by the PD and recorded by the ESA with a resolution bandwidth of 10 Hz over a frequency span of 200 kHz from 79.9 MHz to 80.1 MHz, as shown in Fig. 6(a). The fitting correlation coefficient R^2 is 0.96074, which agrees well with the measured data. The unavoidable 1/f noise of long fiber cavity results in a Gaussian broadening at the center frequency and a theoretical resolution limit of the measurement system is about 4 kHz. Therefore, the laser linewidth is estimated through the 20-dB spectral width of the Lorentz line shape fitting curve to minimize the influence of noise. The 20-dB bandwidth of this proposed laser is 14.02 kHz, and the corresponding 3-dB bandwidth is 701 Hz. In principle, approximately 1000 km delay fiber is required to break the coherence of the beat signal and realize sub-kHz resolution when using Lorentz fitting. However, a long delay fiber is susceptible to noise in the environment and has a large propagation loss, which will adversely affect the linewidth measurement. Here, a 50 km delay fiber is inserted into the DSHI system to measure the laser linewidth. Thus, it will broaden the RF spectrum due to the decoherence of the beat signal and the measured linewidth is larger than the real linewidth. Figure 6(b) shows the 3-dB linewidth of the laser at different wavelengths with Lorentz fitting, ranging from 701 to 975 Hz, which indicates that the Lorentz linewidth of the laser is below 1 kHz. The above results indicate that the tunable single frequency laser can maintain high coherence during the tuning process.

To further confirm the high coherence of the laser, the differential phase noise is characterized by coherent DSHI with a 10-m delay fiber. Here, the laser instantaneous frequency is demodulated using the beat signal with an 80 MHz carrier frequency. The laser wavelength is tuned to 1544.8 nm, and the laser is operated in a SLM under the condition of PT symmetry breaking. The instantaneous frequency evolution of the laser within a time range of 100 ms is shown in Fig. 7(a). The instantaneous frequency of the laser is around ~80 MHz, and there is no obvious jump. Furthermore, the distribution of instantaneous frequency is calculated using the histogram, as shown in Fig. 7(b). The instantaneous frequency of the laser follows normal distribution, which indicates that the laser is greatly affected by random white noise. The full width at half maximum of the frequency distribution is calculated, which shows that the instantaneous frequency jitter of the laser is 15.3 kHz. In addition, the instantaneous frequency evolution and distribution at a wavelength of 1576.1 nm is further measured, as described in 7(c). At this point, the instantaneous frequency jitter of the laser is 28.1 kHz, indicating that the stability of the laser is slightly decreased, as shown in Fig. 7(d). To fully understand the laser instantaneous frequency stability, we measured the instantaneous frequency jitter under different tuned channels, as shown in Figure 7(e). The instantaneous frequency jitter of the laser is less than ~30 kHz, which indicates that the laser has a relatively balanced short-term stability. Figure 7(f) shows the single-sideband frequency noise power spectral density (PSD) curve of the proposed PT symmetric fiber laser obtained by differential phase noise measurement. The frequency noise PSD of the laser and the measurement system noise floor are plotted by the pink curves and gray curves, respectively. The frequency noise level of the laser is higher than the noise floor, which verifies that the characterization of laser frequency noise is credible. Here, the intrinsic linewidth of the laser can be accurately calculated using the effective amplitude of high-frequency white noise derived from spontaneous radiation in the frequency noise PSD, which can

be expressed as $\Delta v = \pi \cdot S_0$, where S_0 is the effective amplitude of highfrequency noise in the PSD spectrum [36]. The white frequency noise limit of the PT symmetric laser is 2.62 Hz²/Hz, which indicates that the intrinsic linewidth is about ~8.2 Hz. Here, the intrinsic linewidth is smaller than the Lorentz linewidth measured with the DSHI method, indicating that the laser is indeed highly coherent. Therefore, the approach of obtaining the intrinsic linewidth of the laser by frequency noise provides guidance for further exploring PTsymmetric optics to achieve high-coherence laser output. Besides, the stability of laser output power is further investigated by using RIN to characterize the power jitter at different frequencies. As shown in Fig. 7(g), the RIN value measured with more than 1 MHz offset frequency range is as low as -140.3 dB/Hz and is higher than the noise floor of the measurement system. The long fiber standing wave cavity is susceptible to quantum noise and thermal noise, which will destroy the equilibrium state of inverted population in the gain medium and cause disturbance of the excited radiation energy in the cavity, thus generating relaxation oscillations to form noise peaks around the ~200 kHz frequency offset in both frequency noise and RIN noise curves.

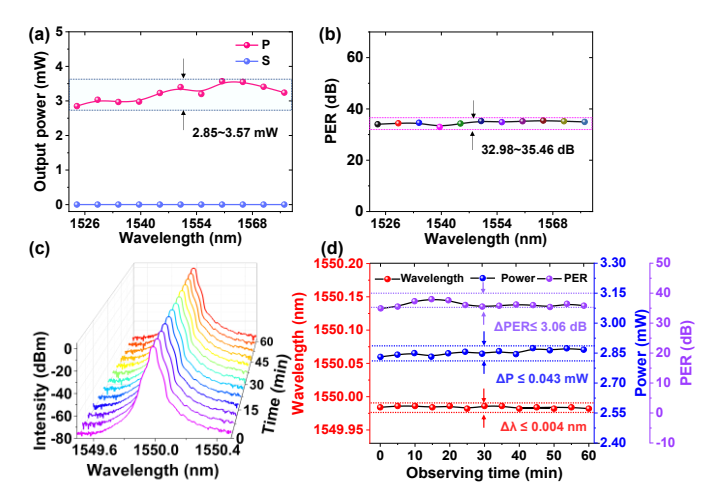


Fig. 8. Linear polarization and long-term stability of the PT symmetric fiber laser. (a) Output power the PBS (P-port and S-port) versus operating wavelength. (b) polarization extinction ratio (PER) in dB as a function of tuning wavelength. (c) Optical spectra of 13 times repeated scans at 5-min intervals. (d) stability performances of the lasing wavelength, output power and PER over 60 minutes.

In particular, the output signal is injected into the PBS with polarization control in the measurement system in Fig. 3 to measure the linear polarization characteristics of the proposed fiber laser. The maximum and minimum output power of P-port and S-port of PBS can be obtained by finely adjusting the PC₃, as shown in Fig. 8(a). The output power of the S-port approaches complete extinction for different wavelengths, the P-port maintains the optimal output power, and the power difference is induced by the uneven gain and loss in the resonant cavity with the wavelength. The PER of the laser output is calculated using the maximum power difference obtained from PBS, as shown in Figure 8(b). The PER is as high as more than 32.98 dB and fluctuates from 32.98 dB to 35.46 dB for different wavelengths. The high extinction ratio is due to the polarizationsensitive FPMR in the laser cavity. Besides, linear polarization is particularly conducive to achieve polarization dependent on PT symmetry condition. To verify the long-term stability of the laser system, the laser output spectra are acquired every 5 minutes for 13 times, as shown in Fig. 8(c). To fully demonstrate the long-term

stability of the PT symmetric tunable fiber laser system, we also monitored the fluctuations of the central wavelength, output power, and PER. Within the 5-minute interval of 60-minute observation, the output power fluctuation is less than 0.043 mW, the central wavelength fluctuation is less than 0.004 nm, and the PER fluctuation is less than 3.06 dB, as shown in Figure 8(d). Here, the maximum output power fluctuation is less than 1.6%, indicating that the proposed scheme has high stability. These experimental results prove that using the PT symmetric mode selection mechanism can ensure high long-term stability when operating at a single frequency and single polarization state.

V. CONCLUSION

In conclusion, we have proposed and experimentally demonstrated an all-fiber tunable Hz-level intrinsic linewidth single-polarization fiber laser based on PT symmetry with a high Q FPMR. The principle of PT-symmetric mode selection for the transition of laser from MLM to SLM is revealed. In the experiment, a single-loop reciprocity system with high-Q FPMR is used to realize PT-symmetric optics, thereby realizing SLM and single polarization operation of linear cavity fiber lasers. In addition, the operating wavelength of the laser can be tuned over a wide range through a TBPF with high stability. The PT symmetric mode selection mechanism has excellent wavelength universality, so that the SMSR is maintained above ~65 dB and the PER is as high as more than 32.98 dB for different wavelengths. Based on the optical delay self-heterodyne methos, a Lorentz linewidth less than 901 Hz is measured. Furthermore, white frequency noise as low as 2.62 Hz²/Hz is measured, corresponding to an intrinsic linewidth of ~8.2 Hz. For offset frequencies exceeding 1 MHz, the measured RIN is as low as -140.3 dB/Hz. In long-term observations, the maximum output power fluctuation is 0.043 mW, the maximum center wavelength fluctuation is 0.004 nm, and the maximum PER fluctuation is 3.06 dB. The proposed PT symmetric mode selection mechanism greatly improves the coherence and stability of the tunable fiber laser, which provides a new perspective for other tunable light sources to achieve single-frequency and single polarization operation.

REFERENCES

- S. Pan, and J. Yao, "A wavelength-switchable single-longitudinal-mode dual-wavelength erbium-doped fiber laser for switchable microwave generation," *Opt. Express*, vol. 17, no. 7, pp. 5414-5419, Mar. 2009.
- [2] C. K. Ha, K. S. Lee, D. Kwon, and M. S. Kang, "Widely tunable ultranarrow-linewidth dissipative soliton generation at the telecom band," *Photonics Res.*, vol. 8, no. 7, pp. 1100-1109, Jul. 2020.
- [3] D. Pan, C. Ke, S. Fu, Y. Liu, D. Liu, and A. E. Willner, "All-optical spectral linewidth reduction of lasers for coherent optical communication," *Opt. Lett.*, vol. 38, no. 24, pp. 5220-5223, Dec. 2013.
- [4] H. Al-Taiy, N. Wenzel, S. Preußler, J. Klinger, and T. Schneider, "Ultranarrow linewidth, stable and tunable laser source for optical communication systems and spectroscopy," *Opt. Lett.*, vol. 39, no. 20, pp. 5826-5829, Oct. 2014.
- [5] Z. S. Liu, B. Y. Liu, S. H. Wu, Z. G. Li, and Z. J. Wang, "High spatial and temporal resolution mobile incoherent Doppler lidar for sea surface wind measurements," *Opt. Lett.*, vol. 33, no. 13, pp. 1485-1487, Jul. 2008.
- [6] D. P. Kapasi et al., "Tunable narrow-linewidth laser at 2 μm wavelength for gravitational wave detector research," Opt. Express, vol. 28, no. 3, pp. 3280-3288, Feb. 2020.

- [7] L. Dang et al., "Tunable ultra-narrow linewidth linear-cavity fiber lasers assisted by distributed external feedback," Opt. Laser Technol., vol. 166, Nov. 2023, Art. no. 109529.
- [8] Y. Li et al., "Tunable narrow-linewidth fiber laser based on the acoustically controlled polarization conversion in dispersion compensation fiber," J. Lightwave Technol., vol. 40, no. 9, pp. 2971-2979, May. 2022.
- [9] L. Dong, W. H. Loh, J. E. Caplen, J. D. Minelly, K. Hsu, and L. Reekie, "Efficient single-frequency fiber lasers with novel photosensitive Er/Yb optical fibers," *Opt. Lett.*, vol. 22, no. 10, pp. 694-696, May. 1997.
- [10] Z. Huang et al., "Self-injection locked and semiconductor amplified ultrashort cavity single-frequency Yb³⁺-doped phosphate fiber laser at 978 nm," Opt. Express, vol. 25, no. 2, pp. 1535-1541, Jan. 2017.
- [11] D. Michel, X. Feng, and K. Alameh, "MEMS-based tunable linear-cavity fiber laser," *IEEE Photon. J.*, vol. 4, no. 3, pp. 895-902, Jun. 2012.
- [12] Q. Yang et al., "Sub-kHz linewidth 1.6-μm single-frequency fiber laser based on a heavily erbium-doped silica fiber," Opt. Lett., vol. 48, vol. 10, pp. 2563-2566, May. 2023.
- [13] Y. Zhang et al., "Ultra-narrow linewidth full C-band tunable single-frequency linear-polarization fiber laser," Opt. Express, vol. 24, no. 23, pp. 26209-26214, Nov. 2016.
- [14] Y. Tao, M. Jiang, C. Li, P. Zhou, and Z. Jiang, "Low-threshold 1150 nm single-polarization single-frequency Yb-doped DFB fiber laser," *Opt. Lett.*, vol. 46. No. 15, pp. 3705-3708, Aug. 2021.
- [15] L. Dang et al., "A longitude-purification mechanism for tunable fiber laser based on distributed feedback," J. Lightwave Technol., vol. 40, no. 1, pp. 206-214, Jan. 2022.
- [16] J. Ji et al., "Narrow linewidth self-injection locked fiber laser based on a crystalline resonator in add-drop configuration," Opt. Lett., vol. 47. no. 6, pp. 1525-1528, Mar. 2022.
- [17] C. Xue, S. Ji, A. Wang, N. Jiang, K. Qiu, and Y. Hong, "Narrow-linewidth single-frequency photonic microwave generation in optically injected semiconductor lasers with filtered optical feedback," *Opt. Lett.*, vol. 43, no. 17, pp. 4184-4187, Sep. 2018.
- [18] A. Regensburger, C. Bersch, M. A. Miri, G. Onishchukov, D. N. Christodoulides, and U. Peschel, "Parity-time synthetic photonic lattices," *Nature*, vol. 488, no. 7410, pp. 167-171, Aug. 2012.
- [19] B. Peng et al., "Parity-time-symmetric whispering-galler microcavities," Nat. Phys., vol. 10, no. 5, pp. 394-398, May. 2014.
- [20] H. Hodaei et al., "Enhanced sensitivity at higher-order exceptional points," *Nature*, vol. 548, no. 7666, pp. 187-191, Aug. 2017.
- [21] J. Zhang, and J. Yao, "Parity-time-symmetric optoelectronic oscillator," Sci. Adv., vol. 4, no. 6, p. eaar6782, Jun. 2018.
- [22] Y. Liu, T. Hao, W. Li, J. Capmany, N. Zhu, and M. Li, "Observation of parity-time symmetry in microwave photonics," *Light-Sci Appl.*, vol. 7, no. 1, p. 38, Jul. 2018.
- [23] J. Zhan, L. Li, G. Wang, X. Feng, B. O. Guan, and J. Yao, "Parity-time symmetry in wavelength space within a single spatial resonator," *Nat. commun.*, vol. 11, no. 1, p. 3217, Jun. 2020.
- [24] H. Hodaei, M. A. Miri, M. Heinrich, D. N. Christodoulides, and M. Khajavikhan, "Parity-time-symmetric microring lasers," *Science*, vol. 346, no. 6212, pp. 975–978, Nov. 2014.
- [25] H. Hodaei et al., "Parity-time-symmetric coupled microring lasers operating around an exceptional point," Opt. Lett., vol. 40, no. 21, pp. 4955-4958, Nov. 2015.
- [26] Z. Dai, Z. Fan, P. Li, and J. Yao, "Widely wavelength-tunable parity-time symmetric single-longitudinal-mode fiber ring laser with a single physical loop," *J. Lightwave Technol.*, vol. 39, no. 7, pp. 2151-2157, Apr. 2020.
- [27] W. Liu et al., "An integrated parity-time symmetric wavelength-tunable single-mode microring laser," Nat. commun., vol. 8, no. 1, p. 15389, May. 2017.
- [28] S. A. Babin, D. V. Churkin, A. E. Ismagulov, S. I. Kablukov, and M. A. Nikulin, "Single frequency single polarization DFB fiber laser," *Laser Phys. Lett.*, vol. 4, no. 6, 428-432, Jun. 2007.
- [29] S. Yamashita, and G. J. Cowle, "Single-polarization operation of fiber distributed feedback (DFB) lasers by injection locking," *J. Lightwave Technol.*, vol. 17, no. 3, pp. 509-513, Mar. 1999.
- [30] L. Hao, X. Wang, K. Jia, G. Zhao, Z. Xie, and S. Zhu, "Narrow-linewidth single-polarization fiber laser using non-polarization optics," Opt. Lett., vol. 46, no. 15, pp. 3769-3772, Aug. 2021.
- [31] X. Cao, J. Zhou, Z. Cheng, S. Li, and Y. Feng, "GHz Figure-9 Er-Doped Optical Frequency Comb Based on Nested Fiber Ring Resonators," *Laser Photonics Rev.*, vol. 17, no. 11, p. 2300537, Nov. 2023.

- [32] Y. Liu et al., "Narrow linewidth parity-time symmetric Brillouin fiber laser based on a dual-polarization cavity with a single micro-ring resonator," Opt. Express, vol. 30, no. 25, pp. 44545-44555, Dec. 2022.
- [33] L. Li, et al., "Polarimetric parity-time symmetry in a photonic system,"
- Light-Sci Appl. vol. 9, no. 1, p. 169, Sep. 2020.
 [34] Z. Fan, Z. Dai, Q. Qiu, and J. Yao, "Parity-time symmetry in a single-loop photonic system," J. Lightwave Technol., vol. 38, no. 15, pp. 3866-3873, Aug. 2020.
- [35] Y. Lv, et al., "Switchable and tunable orthogonal single-polarization dual wavelength SLM fiber laser based on parity-time symmetric system and PM-FBG," Opt. Laser Technol., vol. 166, Nov. 2023, Art. no. 109695.
- [36] L. B. Mercer. 1/f frequency noise effects on self-heterodyne linewidth measurements. J. Lightwave Technol., vol. 9, no. 4, pp. 485-493, Apr.